



## Mass transfer in fluidized beds of inert particles Part II: Effect of particle size and density

N.A. SHVAB<sup>1</sup>, N.V. STEFANJAK<sup>1</sup>, K.A. KAZDOBIN<sup>1</sup> and A.A. WRAGG<sup>2</sup>

<sup>1</sup>Institute of General & Inorganic Chemistry, Ukrainian National Academy of Sciences, Palladin Avenue, 32/34, Kiev, 03680, Ukraine

<sup>2</sup>School of Engineering and Computer Science, University of Exeter, North Park Road, Exeter, Devon, EX4 4QF, Great Britain

Received 30 March 2000; accepted in revised form 27 June 2000

*Key words:* collision mechanism, electrode, fluidized bed, mass transfer, particle density

### Abstract

The mass transfer rate in fluidized beds of inert particles (FIB) is shown to be dependent on the electrolyte flow velocity and the intensity of particle collisions with the electrode. The influence of particle size and density on the ratio of the magnitude of these two influences on the mass transfer rate in a FIB was studied. Use of particle materials of varying density in an FIB permits variation of the two effects. The influence of collision currents prevails in FIBs of low density materials, and the influence of interstitial velocity is dominant in beds of high density material. The ratio of these factors also depends on the size of particles of the same density. With smaller particle size the influence of collision currents is greater. Smoothing of mass transfer maxima in beds of particles both of small and high density is explained. The results establish a basis for the selection of FIB materials for electrochemical processes.

### List of symbols

$D$	diffusion coefficient ( $\text{cm}^2 \text{s}^{-1}$ )
$d_p$	average particle diameter (cm)
$E_p$	average particle kinetic energy (J)
$i_c$	integral of collision current density ( $\text{mA cm}^{-2}$ )
$i_d$	limiting diffusion current ( $\text{mA cm}^{-2}$ )
$K_d$	mass transfer coefficient ( $\text{cm s}^{-1}$ )
$L$	normalized expansion of the fluidized bed, $L = H/H_0$
$p/q$	power of fractional function
$Sc = v/D$	Schmidt number
$U$	electrolyte linear flow velocity ( $\text{cm s}^{-1}$ )

$U_{\max}$	flow velocity corresponding to maximum mass transfer rate ( $\text{cm s}^{-1}$ )
$U_{\text{mf}}$	minimum fluidization velocity ( $\text{cm s}^{-1}$ )

### Greek symbols

$\delta$	diffusion boundary layer thickness (cm)
$\delta_o$	hydrodynamic boundary layer thickness (cm)
$\varepsilon$	fluidized bed porosity
$\rho_p$	particle material density ( $\text{g cm}^{-3}$ )
$\rho_s$	liquid density ( $\text{g cm}^{-3}$ )
$\rho_{\text{eff}}$	effective particle material density, $\rho_{\text{eff}} = \rho_p - \rho_s$ ( $\text{g cm}^{-3}$ )
$\nu$	dynamic viscosity ( $\text{cm}^2 \text{s}^{-1}$ )

### 1. Introduction

The increase in limiting diffusion current in fluidised beds of inert particles (FIB) is caused by thinning of, and disturbance to, the electrode diffusion boundary layer. The interstitial velocity in a FIB and at the electrode is much higher than outside of the bed zone and the flow is also turbulent [1]. During collisions with the electrode, particles, surrounded by their hydrodynamic boundary layer, introduce a specific microvolume of bulk concentration electrolyte into the near-electrode diffusion layer [2–5].

Mass transfer rates in FIBs depend on the values and ratio of the two main influences, namely, the liquid flow velocity and collisions of particles with the electrode. The interstitial velocity in a bed reaches its maximum value at minimum fluidization conditions, and then remains practically constant in the velocity range corresponding to normal FIB behaviour [4]. The other influence on mass transfer enhancement is particle–electrode collisions. The volume of reagent introduced to the electrode diffusion layer during collision is determined by the thickness of the hydrodynamic boundary layer and the collision frequency [5]. The

latter is determined by the average kinetic energy of the particles. Thus, the magnitudes of both influences on mass transfer in a FIB are determined by the minimum fluidization velocity. This depends on particle size as well as on the electrolyte density and viscosity [5].

The influence of electrolyte viscosity on mass transfer rate in a FIB was investigated recently [6] in aqueous solutions of different viscosity, containing carboxymethylcellulose (CMC), in the range  $1040 < Sc < 3300$ . It was shown that the mass transfer rate decreases as  $Sc$  increases. This resulted from the reduction in effective particle density,  $\rho_{\text{eff}} = \rho_p - \rho_s$ , with increase in the CMC concentration. The maximum in mass transfer rate in solutions of various viscosity was observed in the interval  $0.5 < \varepsilon < 0.6$  [6], which correlates with the maximum particle kinetic energy [7]. The average particle kinetic energy,  $E_p$ , was shown to be dependent on the hydrodynamic parameters of the fluidized bed and is given by the following equation [7]:

$$E_p = 9.13 \times 10^{-6} (U/\varepsilon)^{0.66} \rho_{\text{eff}}^{0.38} d_p^{0.66} v^{0.28} \quad (1)$$

where  $E_p$  is calculated in joules.

As the viscosity and density of electrolytes, especially when dilute, change little,  $Sc$  is of order 1000 in most cases [8, 9]. Thus, the main parameters influencing the mass transfer rate are the particle size and density. In a FIB the thickness of the diffusion boundary layer is related to the thickness of the hydrodynamic boundary layer by the relationship:

$$\delta = \delta_0 Sc^{-1/3} \quad (2)$$

which is valid for any degree of fluidization [8]. Thus, from Equation 2  $\delta_0 \approx 10 \delta$ .

It is obvious that the mass transfer rate in a FIB is fundamentally determined by hydrodynamic factors, related to particle size and density. In accordance with Equation 1, the mass transfer rate should increase with particle size and density. In reality, the logarithm of the mass transfer coefficient maximum is proportional to the logarithm of particle diameter [10]. Thus, the flow velocity corresponding to the maximum mass transfer rate,  $U_{\text{max}}$ , is related to particle size by the equation:

$$U_{\text{max}} = 23.3 d_p^{0.7} \quad (3)$$

The maximum mass transfer rate is reached in the bed porosity range  $0.5 < \varepsilon < 0.6$  [6–8]. This interval was shown to be characteristic of glass particles of  $\rho_{\text{gl}} \approx 2.5 \text{ g cm}^{-3}$  only. Thus, it was necessary to study the influence of particle size and density on the ratio of their influences on mass transfer rate in a FIB.

## 2. Experimental details

Much of the experimental installation was as described earlier [5]. However, planar and cylindrical electrodes

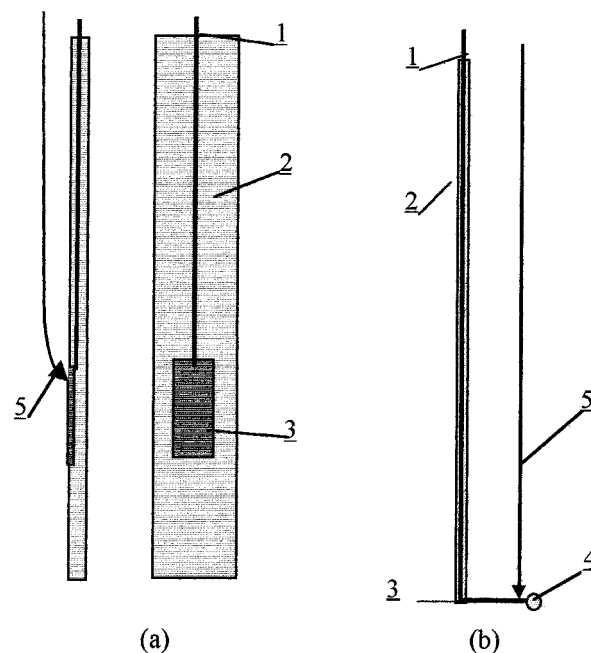


Fig. 1. Electrode arrangements: (a) planar electrode; (b) cylindrical electrode. Key: (1) connection; (2) insulating support; (3) exposed electrode; (4) insulating Pyrex bulb; (5) Luggin capillary.

were used instead of the point electrodes used in [5]. A diagram showing the electrode placement is shown as Figure 1.

The planar working electrode was a platinum plate ( $S = 2 \text{ cm}^2$ ) with its surface flush mounted with a vertical Plexiglass plate (the electrode support). The electrode was fixed using epoxy cement and was ground and polished flush with the plate. The electrode, in its support plate, was positioned facing the diaphragm at a vertical distance of 10 cm from the flow distributor.

The cylindrical electrodes ( $L = 20 \text{ mm}$ , and diameter 0.5; 1.0 and 2.0 mm, respectively) were made of Platinum wire bent at an angle normal to the supporting contact, and insulated by means of welding into a Pyrex tube. The end of the electrode was also isolated by means of a Pyrex bulb. The electrodes were placed normal to the electrolyte flow, together with an attached Luggin capillary, in the bulk of the bed at a distance of 10 cm from the flow distributor.

The electrochemical measurements were made using a PI-50-1 potentiostat and were recorded on a LKD-4 potentiometer. The limiting diffusion currents for copper ion reduction in fluidized beds of particles of various size and density were measured in a manner similar to that in [11–14].

Spherical granules of copper of density ( $\rho_{\text{Cu}}$ ) of  $8.9 \text{ g cm}^{-3}$  and granules of soft-acid ion-exchange resin KB-4, analogous to Amberlyte IRC-50 ( $\rho_{\text{IEM}} = 1.25 \text{ g cm}^{-3}$ ) were used.

The surface of the copper granules was insulated by oxidation at  $600 \text{ }^\circ\text{C}$ . The non-conducting nature of the surface of the granules was confirmed in each case by means of preliminary electrolysis. The experiment was

valid if no copper deposition occurred on the Cu granules. Studies were conducted in electrolyte containing  $3.15 \times 10^{-3}$  M  $\text{Cu}^{2+}$  with 0.75 to 1 M  $\text{Na}_2\text{SO}_4$  (pH 2.5 to 3). Since 4 l of electrolyte were used variations in concentration during an experiment were small. Also, after each measurement the deposit of copper was anodically dissolved so that the bulk concentration was maintained constant over a long time scale.

The granules of ion-exchange resin were previously saturated with copper ions from solution containing 0.5 M  $\text{Cu}^{2+}$ , pH 3, and rinsed in deionized water before each experiment. The value of  $\text{p}K_a$  for KB-4 ion exchanger is known to be in the region 3.9 to 4.0 [15]. Studies were conducted in rather concentrated electrolyte, containing 0.1 M  $\text{Cu}^{2+}$ , pH 2.5, lower than  $\text{p}K_a$ . These experimental conditions render the influence of ion exchange on the limiting diffusion current negligible.

All the experiments were carried out at  $20 \pm 2$  °C.

### 3. Results and discussion

The dependence of limiting current for  $\text{Cu}^{2+}$  reduction on the flow velocity for a FIB of ion-exchanger resin granules is shown in Figure 2(a). Comparison of the dependencies of mass transfer rate on flow velocity for particles of small density and glass particles [6–8] has shown that mass transfer to an electrode in a bed of light particles has some characteristic features. The fluidization begins at extremely low flow rates in comparison with glass particles; in the order of  $0.1 \text{ cm s}^{-1}$ . A maximum limiting current value is reached at a value of  $L (H/H_0)$  of approximately 1.7. The sharp maximum of limiting current, characteristic of beds of glass particles, is absent.

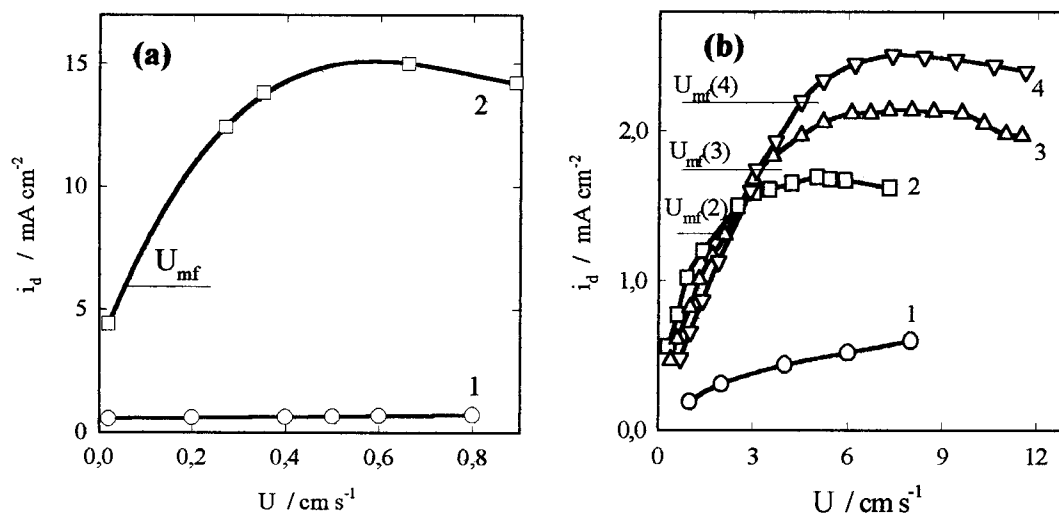


Fig. 2. Dependence of limiting current for  $\text{Cu}^{2+}$  reduction on electrolyte flow velocity in electrolyte flow alone (curve 1) and in a FIB of particles of different density. (a) Granulated ion-exchange resin KB-4; curve 2:  $d_p = 0.07$  cm,  $\rho_p = 1.25$  g  $\text{cm}^{-3}$ . (b) copper granules; curves 2, 3, 4:  $d_p = 0.055$ ,  $0.09$  and  $0.125$  cm, respectively,  $\rho_p = 8.9$  g  $\text{cm}^{-3}$ . Electrolyte: (a)  $0.1$  M  $\text{Cu}^{2+}$ ,  $0.75$  M  $\text{Na}_2\text{SO}_4$ , pH 3. (b)  $3.15 \times 10^{-3}$  M  $\text{Cu}^{2+}$ ,  $1.0$  M  $\text{Na}_2\text{SO}_4$ , pH 2.5.

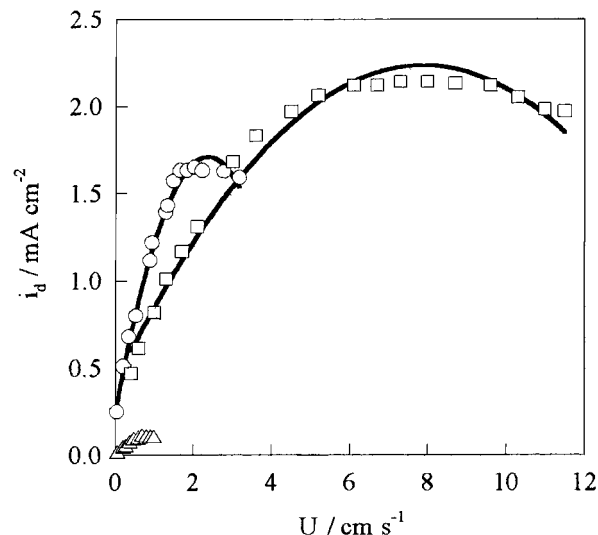


Fig. 3. Dependence of limiting current for  $\text{Cu}^{2+}$  reduction on electrolyte flow velocity in a FIB of particles of different density. Key: ( $\Delta$ ) particles of ion-exchanger; ( $\circ$ ) glass particles; ( $\square$ ) insulated copper granules.  $d_p = 0.09$  cm. Recalculated for the electrolyte containing  $3.15 \times 10^{-3}$  M  $\text{Cu}^{2+}$ ,  $1.0$  M  $\text{Na}_2\text{SO}_4$ , pH 2.5.

Though at minimum fluidization velocity the limiting diffusion current for the particles of ion-exchange resin is higher than in flow without particles ( $i_{mf}/i_{ec}^{mf} \approx 1.8$ ), the influence of the interstitial velocity [5] is less than in the bed of glass particles of the same size. Thus, the influence of collision currents,  $i_c/i_d$ , increases to 70% (Figure 3). This results from the decrease in minimum fluidization velocity, which leads to an increase in hydrodynamic boundary layer thickness. The thickness of the diffusion layer and the volume of reagent introduced during collision,  $\Delta V$ , [5] thus increase.

The dependence of limiting current on flow velocity for the FIB of insulated copper granules is shown in Figure 2(b). In this bed of heavier particles the limiting

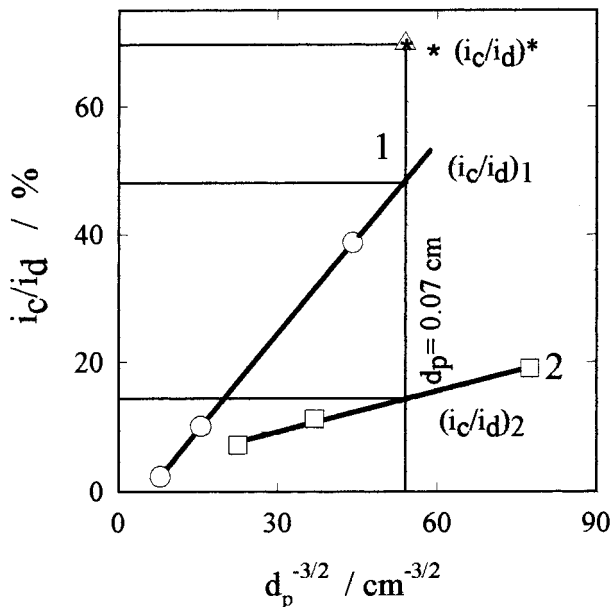


Fig. 4. Dependence of percentage influence of collision on particle size and density. Key: (○) spherical glass beads,  $\rho_p = 2.5 \text{ g cm}^{-3}$ ; (□) insulated copper granules,  $\rho_p = 8.9 \text{ g cm}^{-3}$ ; (\*) granulated ion-exchange resin KB-4,  $\rho_p = 1.25 \text{ g cm}^{-3}$ . Calculated for  $3.15 \times 10^{-3} \text{ M Cu}^{2+}$ .

currents increase due to the greater influence of the interstitial velocity. At the same time, a decrease in diffusion layer thickness occurs (Figure 5(a)), and the influence of collision currents decreases (Figure 4). This explains the absence of the sharper maximum on the dependencies of mass transfer rate on velocity obtained for FIBs of particles of higher density (Figure 2(b)).

Comparison of mass transfer rates in FIBs of particles of identical size but of varying density, expressed in terms of  $K_d$ , has shown (Figure 5(b)), that a two fold increase in material density (from ion-exchanger to glass

granules) results in a more than threefold increase in mass transfer rate. This increase in process intensity, obtained for a small increase in the energy consumption required for fluidization, is noteworthy.

However, further increase in particle density does not result in the expected concomitant increase in mass transfer. The reason is that the interrelation between the mass transfer rate obtained at optimum degree of fluidization and the solid phase density, as well as appropriate flow velocity, have a nonlinear character. According to available known data the functional relationship is of the form (Figure 6):

$$y = x^{p/q}, \quad (4)$$

where  $0 < p/q < 1$ . This arises from the non-linearity of the dependence of minimum fluidization velocity on particle density.

Understanding the role of the hydrodynamic factors affecting the electrode process in a FIB allows an economically sound choice of particle material to be made. The energy required to maintain a desired flow is proportional to the square of the velocity. Approximately the same mass transfer rates are found in FIBs of glass and copper granules with average particle diameters of 0.08 cm and 0.055 cm, respectively. However, though the glass particles are 1.5 times larger, to maintain a bed of Cu particles in the fluidised state, requires a 1.7 times larger flow velocity with the consequent increased energy demand. On reduction of the particle size down to approximately 0.035 cm the advantage of the heavier particles disappears. It is clear that the use of heavy inert particles ( $> 4 \text{ g cm}^{-3}$ , Figure 6(a)) in, for example, metal electrowinning, is unreasonable from an economic point of view.

In the FIB of light resin particles, the limiting current reaches more than 70% of the maximum in the initial

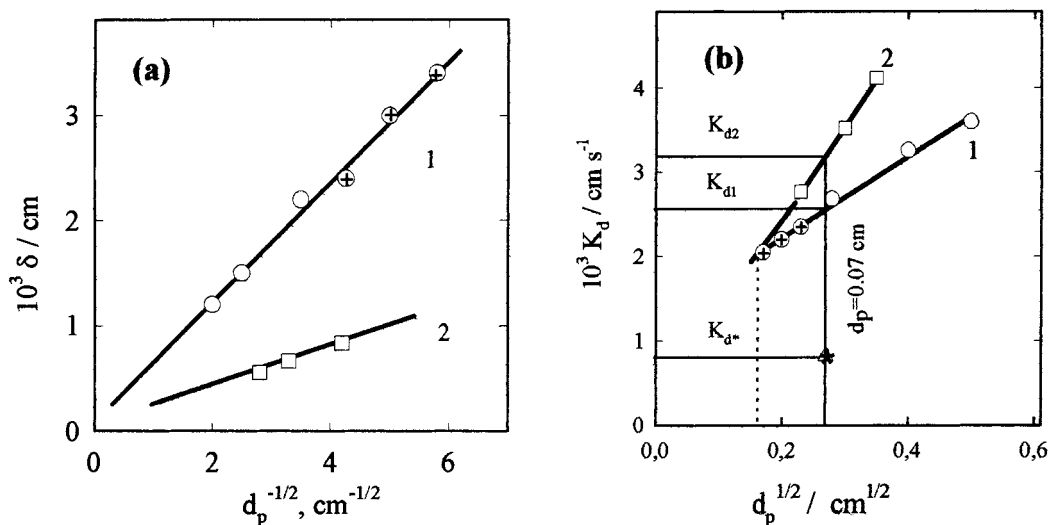


Fig. 5. Dependence of diffusion layer thickness (a) and  $K_d$  (b) on size and density of particles.  $L = L_{opt} = 1.5$ . Key: (○) spherical glass beads,  $\rho_p = 2.5 \text{ g cm}^{-3}$ ; (⊕) data from [13]; (□) insulated copper granules,  $\rho_p = 8.9 \text{ g cm}^{-3}$ ; (\*) granulated ion-exchange resin KB-4,  $\rho_p = 1.25 \text{ g cm}^{-3}$ ,  $d_p = 0.07 \text{ cm}$ .

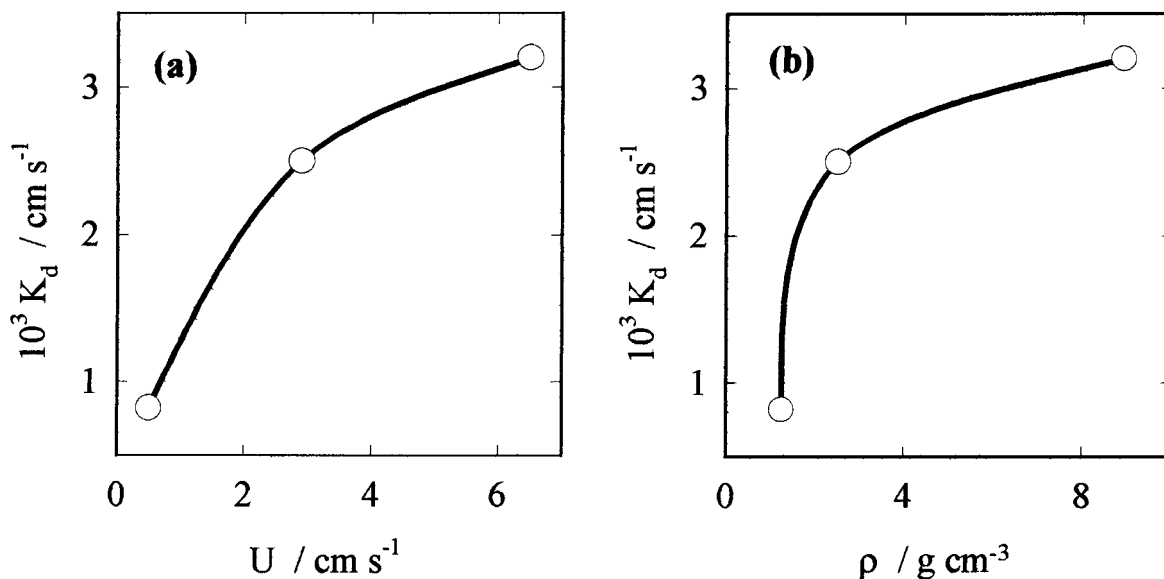


Fig. 6. Dependence of mass transfer coefficient  $K_d$  on (a) velocity and (b) particle density. Average particle diameter:  $d_p = 0.07$  cm;  $L = L_{opt} = 1.5$ .

degrees of fluidization ( $L \approx 1.2$ ). Since the ion-exchanger granules are inclined to elutriation due to their small effective density ( $\rho_{eff} = \rho_p - \rho_s = 0.25$  g cm $^{-3}$ ), such particles must be used at flow velocities only slightly exceeding the fluidization velocity. The use of ion-exchange materials, in spite of the relatively small energy consumption for fluidization, is also inappropriate because of the small mass transfer rates obtained. However, such materials are appropriate when their ion-exchange properties are used, as, for example in [17].

The evaluation of electrolysis efficiency in FIBs, permits identification of an economically optimum particle size. The comparison of mass transfer rates for glass particles, achieved in FIBs of various size fractions and resultant fluidization velocities, shows that the optimum size for glass particles is  $0.10 < d_p < 0.12$  cm. This is also confirmed by data on mass transfer to cylindrical electrodes of different diameter in an FIB (Figure 7).

As shown in Figure 7, in the particle diameter range 0.08 to 0.18 cm, the mass transfer rate increases proportionally to the square root of particle diameter. Further increase in particle size results in deviation from this relationship and little further increase in mass transfer rate. This may be explained by the distinctive features of the flow structure around the cylindrical electrode and the resultant particle circulation patterns [18].

#### 4. Conclusions

It is clear that the use of particles of materials of different density in FIBs allows variation of the contributory influences on mass transfer. In FIBs of materials of low density the influence of collisions

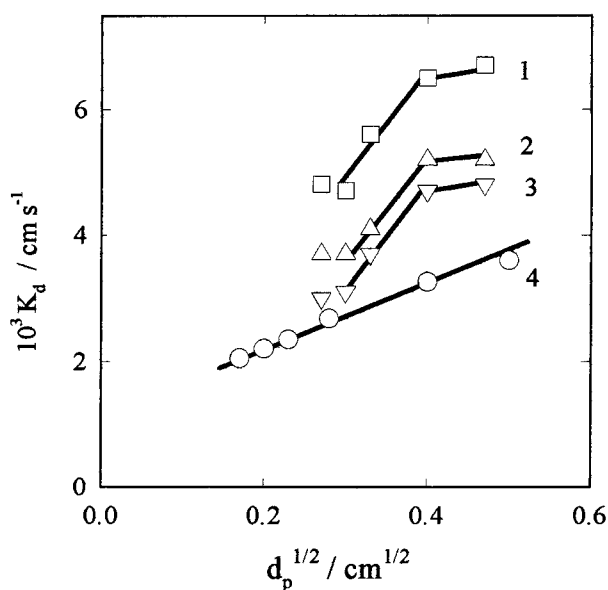


Fig. 7. Dependence of mass transfer coefficient to cylindrical electrodes on particle diameter.  $\rho_p = 2.5$  g cm $^{-3}$ ,  $L = 1.5$ . Curves: (1, 2, 3) cylindrical electrodes of 0.5, 1.0 and 2.0 mm diameter, respectively; (4) planar electrode. Electrolyte:  $5 \times 10^{-2}$  M Cu $^{2+}$ , 1.0 M Na $_2$ SO $_4$ , pH 3.

prevails and in beds of high density the influence of interstitial velocity dominates. The ratio of the influences changes with reduction in the size of particles of the same density, since with reduction of particle size the influence of collision currents increases. These phenomena explain the smoothing of mass transfer maxima in beds of particles of both small and high density. The results obtained permit a sound choice of FIB particle material for different electrochemical processes and the calculation of mass transfer rates both in inert and conductive fluidized beds [5, 19].

**References**

1. F.B. Leitz and L. Marincic, *J. Appl. Electrochem.* **7** (1977) 473.
2. R.H. Muller, D.J. Roha and C.W. Tobias, 'Transport Processes in Electrochemical Systems' (edited by R.S. Yed, T. Katan and D.-T. Chin), Electrochemical Society, Pennington, NJ (1982), p. 1.
3. N.A. Shvab, N.V. Stefanjak, E.I. Kondruk, V.A. Sobkevich and K.A. Kazdobin, *Ukr. Khim. Zh.* **56** (1990) 1057.
4. N.A. Shvab, A.V. Gorodyskii and V.A. Sobkevich, *Elektrokhimiya* **19** (1983) 800.
5. N.A. Shvab, N.V. Stefanjak, K.A. Kazdobin and A.A. Wragg, *J. Appl. Electrochem.* (2000), accepted.
6. F. Coeuret and P. Le Goff, *Electrochim. Acta* **21** (1976) 195.
7. J. Bordet, P. Le Goff and F. Vergnes, *Powder Technol.* **5** (1971/72) 365.
8. P. Le Goff, F. Vergnes, F. Coeuret and J. Bordet, *Ind. & Eng. Chem.* **61** (1969) 8.
9. B. Levich, 'Physico-chemical Hydrodynamics' (Prentice Hall, New York, 1964).
10. G. Kreysa, S. Pionteck and E. Heitz, *J. Appl. Electrochem.* **5** (1975) 305.
11. N.A. Shvab, E.I. Kondruk and A.Ya. Aguzhen, *Ukr. Khim. Zh.* **51** (1985) 170.
12. N.A. Shvab, N.V. Stefanjak and K.A. Kazdobin, *Ukr. Khim. Zh.* **58** (1992) 487.
13. A.T.S. Walker and A.A. Wragg, *Electrochim. Acta* **25** (1980) 323.
14. K. Bouzek, J. Palmer, I. Rousar and A.A. Wragg, *Electrochim. Acta* **41** (1996) 323.
15. V.N. Startsev, V.V. Yatsuk and L.N. Stepanova, *Tsvetnye Metally* (1971) 22.
16. A.D. Davydov and G.R. Engelhardt, *Elektrokhimiya* **24** (1988) 3.
17. R. Tison, *Plat. Surf. Finish.* **75** (1988) 114.
18. N.A. Shvab, N.V. Stefanjak and K.A. Kazdobin, *Ukr. Khim. Zh.* **58** (1992) 487.
19. N.A. Shvab, A.V. Gorodyskii and K.A. Kazdobin, *Elektrokhimiya* **22** (1986) 147.